JCTC Journal of Chemical Theory and Computation

Article

pubs.acs.org/JCTC

Simulations of Adiabatic Electrochemical Reduction of the CF_3I Molecule—Assessment of Different Models

Anna Ignaczak*

Department of Theoretical and Structural Chemistry, University of Lodz, ul. Pomorska 163/165, 91-236 Łódź, Poland

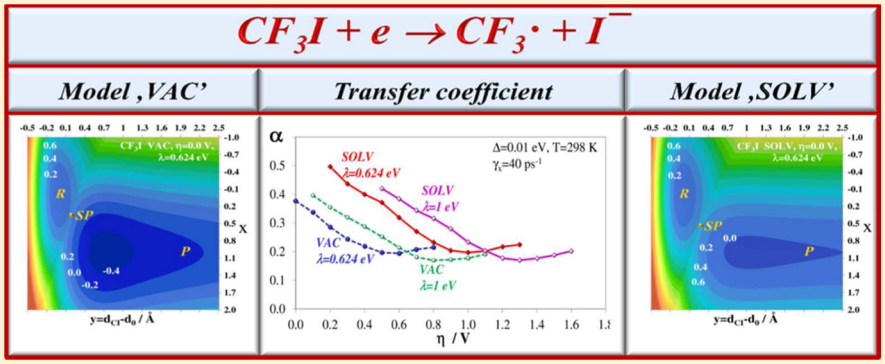

ABSTRACT: The kinetics and mechanism of electrochemical reduction of the CF_3I molecule are studied using molecular dynamics simulations. The potential energy surface used in the simulations is based on the Newns−Anderson−Schmickler Hamiltonian and on the analytical potentials fitted to points obtained from quantum calculations for the CF_3I neutral molecule and anion. Two different sets of points were used for fitting: the first obtained in vacuo[1] and the second in dimethyl sulfoxide,[2] which yields two models, named respectively "VAC" and "SOLV." Additionally, each model was tested with two different values of the solvent reorganization energies: λ = 0.624 eV and λ = 1 eV. The results show that both models provide results which are qualitatively similar but differ quantitatively, mainly due to a shift in the overpotential η. The electron transfer coefficient is found to vary linearly at a certain range of overpotentials, but this relation changes for larger η, where it takes a parabolic-like form. The transfer coefficient is very sensitive to the λ value: at T = 298 K and η = 0.9 V, we report values α = 0.204 obtained for λ = 0.624 eV and α = 0.28 for λ = 1 eV.

1. INTRODUCTION

Halogenated fluorocarbons for many years have attracted the attention of scientists for two reasons: first, they were found in the past to be very useful in many industrial areas, for example as fire extinguishing materials, refrigerants, or chemical etchants. On the other hand they are known as ozone-depleting substances; thus, after a period of very intense production, the investigations were focused on finding an inexpensive and possibly useful method for their disposal. Despite their bad fame, halogenated fluorocarbons still find various applications;[3−17] for example, they can be very useful in the etching of surfaces, synthesis of organometallic compounds, and perfluorination reactions.

As demonstrated in several recent works,[3−7,11−13,16] electrochemical activation of trifluoromethyl halides can be successfully used in the above-mentioned processes. The most comprehensive study on the electrochemical reduction of various halogenated organic compounds was given in a series of works by Savéant and co-workers.[18−27] Among the chemicals studied were also CF_3Br and CF_3I molecules, for which the reduction potentials were measured at different electrodes: glassy-carbon, Pt, Au, Hg, stainless steel, Ni, and Cu.[21−23] For the reduction on a glassy carbon electrode, additionally the transfer coefficients were obtained at a given potential.[21]

Electrochemical reduction of CF_3X molecules was studied also by other authors. The reduction potentials and several electrode materials for the reduction of CF_3Br very recently were re-examined by Grobe and Hegge.[16] In the works of Sonoyama and Sakata, the reduction of CF_3Cl at 13 different metals in the 1:1 mixture of water and methanol,[12] as well as at the Ag electrode in acetonitrile and additionally in the presence of carbon dioxide,[13] was investigated as a method of conversion of trifluoromethyl chloride into other compounds. In the work of Rozhkov et al.,[28] the potential of electrochemical reduction of CF_3I on Pt in CH_3CN was reported. Electroreduction of the same molecule also in acetonitrile, but on a glassy carbon electrode, in the absence and the presence of cobaloximes was studied by Volodin et al.[29]

The essential step in such reactions is the transfer of an electron from the electrode to the neutral CF_3X (X = Cl,Br,I) molecules, which in solutions occurs with the simultaneous rupture of the C−X bond and formation of the radical CF_3 and anion X^-. Theoretical investigations of these processes are mostly focused on selected properties of substrates and products in the gas-phase;[1,30−51] very few take into account

Received: May 18, 2013
Published: September 3, 2013

   dx.doi.org/10.1021/ct400411v | J. Chem. Theory Comput. 2013, 9, 4304−4312

the solvent effect.[2,24,52] For the analysis of the reaction mechanism the most important works are those providing potential energy profiles (PES) of the neutral molecules and anions with respect to the C−X bond dissociation. In the article of Bertran et al.[24] the PES obtained at the MP2/4-31G* level for the CF_3Cl and CF_3Cl^- molecules in the gas phase and in the polar solvent, introduced via the polarizable continuum model (PCM) with dielectric constant $\varepsilon = 37$, were presented. In two subsequent works, German and Tikhomirov studied the energy profiles of several polyhalogen methanes, including CF_3Cl and CF_3Br, in the absence[51] and the presence of a solvent,[52] using the semiempirical method PM3.

Very recently, my co-worker and I performed the density functional PBE1PBE/aug-cc-pVTZ calculations of the PES for the neutral and reduced forms of CF_3X (X = Cl,Br,I) in vacuo.[1] In my later work,[2] the same method was combined with the PCM model to analyze the solvent effect on the potential energy profiles of these molecules in argon, acetonitrile (ACN), and dimethyl sulfoxide (DMSO), as well as on the height of the energy barrier for the reductive bond cleavage. All works comparing the potential energy curves of the molecule and anion in vacuo and in solution concluded that the solvent has a minor effect on the C−X interaction in the neutral molecule but is quite strong in the anion. However, due to the inability to verify the results obtained with the PCM model, it is difficult to judge their accuracy.

In all above-mentioned works, the reaction mechanism was analyzed in the homogeneous environment; thus they are only indirectly related to the electrochemical reduction. As shown in a series of our earlier works,[53−56] the potential energy profiles obtained from quantum calculations, combined with the earlier theory of Schmickler describing a heterogeneous electron transfer, yield the model which can be applied to study the kinetics and mechanism of such reactions. This strategy was successfully used for studies on the electrochemical reduction of *tert*-butyl chloride and bromide. In those early works, the potential energy profiles were based on the results obtained in vacuo, which was justified by the small energy of stabilization of the anion.

In the following article, I present the application of this model to analyze the adiabatic reduction of trifluoromethyl iodide on an electrode. This particular molecule is chosen because its electrochemical activation is the easiest among the three trifluoromethyl halides, requiring the smallest overpotential, thus allowing the exploration of also the potential range close to equilibrium. Due to some uncertainty about the proper description of the solvent via the PCM model, the results obtained from quantum calculations in vacuo and in solution are treated in this work as two borderline cases, yielding different potential energy surfaces. Selected results obtained with the two models are compared to electrochemical data for this system given in the literature, which serves to verify the quality of both approaches.

2. METHOD

2.1. General Description of the Model. The theoretical model used in the present work is described in detail in our earlier works;[53−56] therefore only essential information is provided below. There are two important parts forming it—the potential energy surface (PES) and the simulation algorithm. The former is derived from the model Hamiltonian, which in its general form was proposed by Koper et al.[57,58] There is an important assumption in the model Hamiltonian, namely that the reduced molecule is not specifically adsorbed on the metal surface and thus is separated from it by at least one layer of solvent molecules. Within this approximation, the Hamiltonian takes into account three key elements of the process of electrochemical reduction: H_e, the interaction between electronic states on the reactant and on the electrode; H_{ph}, reorganization of the solvent; and H_{bb}, intramolecular changes of the reactant. In H_e, the electronic states of the reactant and metal are described by their energies ε and number operators n, and an additional term accounts for the electron exchange between them. The solvent in H_{ph} is modeled as a phonon bath linearly coupled to the electron transfer via n_a, the occupation number of the antibonding orbital of the reactant. The last part of the model Hamiltonian, H_{bb}, depends on specific properties of the reactant, and in the case of the bond-breaking electron transfer, it reflects energy changes related to the bond stretching and its dissociation upon reduction. It contains expressions for the potential energies $V_i(y)$ and $V_f(y)$ of the initial and final states (before and after reduction), respectively, where y denotes elongation of the dissociating bond with respect to its equilibrium value in the neutral molecule. As in H_{ph}, also here the occupation number n_a is used to switch from the initial to the final state: $H_{bb} = (1-n_a)V_i(y) + n_aV_f(y)$.

From this model Hamiltonian, the ground-state adiabatic potential energy surface can be obtained using several further approximations. First, it is assumed that the energy evolution related to the solvent reorganization during reaction can be expressed in terms of only one generalized coordinate x, which is dimensionless and normalized such that $x = 0$ corresponds to the energy minimum at the initial state (before the electron is transferred to the particle), while $x = 1$, to the energy minimum at the final state (after reduction). In this approach, well-known from the Marcus theory, the solvent response is represented by the reorganization energy λ. Another simplification comes from the wide-band approximation, in which the interaction between the electronic states on the reactant and metal is described by the energy broadening parameter Δ, which is assumed to be constant.

The final form of the PES for the dissociative electrochemical reduction is as follows:

$$E(x, y) = \tilde{\varepsilon}_a\langle n_a\rangle + \lambda x^2 + \frac{\Delta}{2\pi}\ln\left(\frac{\tilde{\varepsilon}_a^2 + \Delta^2}{\varepsilon_a^2 + \Delta^2}\right) + V_i(y) \quad (1)$$

where

$$\tilde{\varepsilon}_a(x, y) = \varepsilon_a - 2\lambda x + V_f(y) - V_i(y) \quad (2)$$

is the electronic energy obtained by collecting all terms containing the occupation number defined as $\langle n_a\rangle = (1/\pi)\mathrm{arccot}(\tilde{\varepsilon}_a/\Delta)$. ε_a is the energy of the antibonding orbital calculated with respect to the Fermi level, and for the bond-breaking reactions it has the form $\varepsilon_a = \lambda - e_0\eta$, where η is the effective overpotential. As can be seen, the potential energy surface E is thus a function of two effective variables (x and y) and contains additionally three parameters (λ,Δ,η) influencing the reduction process. Of course, the shape of the PES will depend also on the potentials V_i and V_f describing the dissociation of the C−I bond in the CF_3I molecule and anion.

2.2. Potentials for Intramolecular Reorganization of the Reactant. As stated already, in the present work two different models of V_i and V_f are tested as components of the potential $E(x,y)$—the first is based on the energy profiles obtained from the quantum calculations performed at the

dx.doi.org/10.1021/ct400411v | J. Chem. Theory Comput. 2013, 9, 4304−4312

PBE1PBE/aug-cc-pVTZ level for the CF_3I and CF_3I^- in vacuo[1] and the second on similar calculations performed in the presence of DMSO.[2] In both works,[1,2] the quality of results obtained with the PBE1PBE/aug-cc-pVTZ method in vacuo and in several solvents was carefully verified for the CF_3X systems (X = Cl, Br, I) by comparing selected results (structural properties, electron affinities, vibrational frequencies, dissociation energies) with values obtained with the quantum chemistry composite methods, with experimental data, as well as with results reported in earlier theoretical works. In the second work, some additional qualitative validation of the results obtained with the PCM model was made for the CF_3Cl^- anion at the PBE1PBE/6-31+G* level using the cluster model approach (the anion was surrounded by 12 acetonitrile molecules). As shown in the latter work, the PCM model gives almost identical results for two solvents, ACN and DMSO; therefore we will distinguish the two approaches by using notations "VAC" and "SOLV," bearing in mind that they refer only to results of quantum calculations.

It is suitable to express V_i and V_f as analytical functions fitted to the points obtained from quantum calculations. In both models, these analytical potentials are assumed as combinations of exponential terms, and for the neutral molecule they have the same form:

$$V_i(y) = A_1 \exp(-A_2 y) + A_3 \exp(-A_4 y) + A_5 \exp(-A_6 y) + A_7 \quad (3)$$

The bond stretching y is defined as $y = d_{CI} - d_0$, where d_{CI} denotes the actual length of the C−I bond in CF_3I, and d_0 is its equilibrium value in the neutral molecule. Thus, the minimum of the function V_i in both models corresponds to $y = 0$ Å. The parameters A_i are obtained from fitting, separately for each model.

Similar functions are used for the anion CF_3I^-, but in this case some differences in the shape of the curves obtained in vacuo and in solvent have to be accounted for. Thus, in the model VAC, the following potential is fitted:

$$V_f(y') = B_1 \exp(-B_2 y') + B_3 \exp(-B_4 y') + B_5 \exp(-B_6 y') + B_7 \exp(-B_8 (y' + d_2)^2) \quad (4)$$

where $y' = d_{CI} - d_1 = y - d_1 + d_0$; d_{CI} here denotes the actual length of the C−I bond in CF_3I^-, d_0 is the equilibrium C−I distance in the neutral molecule CF_3I, d_1 is the equilibrium C−I distance in the anion CF_3I^-, and d_2 is an additional parameter introduced to improve the quality of fitting. In the model SOLV, the last term in eq 4 is omitted; thus only six parameters B_i are needed. The results of fittings for both cases and the corresponding PES will be presented in section 3.1.

2.3. Simulation Method. The potential energy surface $E(x,y)$ was next incorporated in our simulation program, which is based on the stochastic collision model of Kast et al.[59,60] This method was successfully used in our earlier studies on the kinetics of reduction of other systems;[54−56,61,62] among them were also bond breaking reactions. The Kast et al. model assumes that the system particle 1 collides randomly with the particles 2 of the heat bath, which is taken to be infinitely large. The motion of the system particle is then described by the modified Verlet algorithm, in which the new position r_{n+1} of particle 1 in one dimension is expressed as

$$r_{n+1} = (2 - \alpha) r_n - r_{n-1} + \alpha r_{n-2} + 2\alpha u_n dt + a_s (dt)^2 \quad (5)$$

Here, a_s is an acceleration of the particle, dt is the time step, and u_n is a velocity of the bath particles at the temperature T described by the Maxwell−Boltzmann distribution equation. The parameter α is the mass ratio $\alpha = m_2/(m_1 + m_2)$, where m_1 and m_2 are masses of the particles 1 and 2, respectively. For relatively small α and dt, the "friction" γ exerted by the bath on the particle can be then expressed as $\gamma = 2\alpha/dt$.

The potential energy surface $E(x,y)$ is a function of two variables; therefore this algorithm was applied to each direction separately. Since the longitudinal relaxation time of common solvents is usually on the order of 1 ps, the frequency ω_x was assumed to be equal to 1 ps^{-1}. Using harmonic oscillator approximation and taking into account that the coordinate x is dimensionless, the mass m_x can be easily derived, giving $m_x = 2\lambda$. For the mass m_y, the value of 44.7 atomic mass units was used, which is the reduced mass of the CF_3 and I fragments.

Since the frequency ω_y is much higher than ω_x, in the simulations two different time scales were defined, with the time-steps fulfilling the relation: $dt_x/dt_y = \omega_y/\omega_x = 54$. In all simulations, the time-step dt_x was set to be equal to 0.01 ps. Additionally, as discussed in our earlier works and also in the literature,[63−65] an effect of the delayed response of the solvent in the y direction, and thus a smaller friction exerted on the C−I bond (due to its fast vibration), should be accounted for, and this was done by using the simple relation $\omega_y/\omega_x = \gamma_x/\gamma_y$.

The rate k of the reaction occurring at given conditions was then calculated as the inverse of the average time required by the system to escape from the reactant well to the product area. Depending on the barrier height, the averaging was made over 1000−4000 trajectories. Each single simulation started at the bottom of the initial state well (R) and ended when the electron was entirely transferred to the reactant. The latter was defined by the numerical condition for the occupation probability: $n_a > 0.99$.

3. RESULTS

3.1. Potential Energy Surfaces. The parameters obtained from the fitting of analytical functions described in section 2.2 are given for both models in Table 1, and the corresponding potential curves V_i and V_f are shown along with quantum points in Figure 1. As can be seen, the fitted potentials correctly reproduce the shape of energy profiles, their minima, and the crossing points of the potential energy curves for the neutral molecule and the anion. The latter defines the height of the barrier for the C−I bond dissociation upon reduction, which, according to the quantum calculations, is much higher in solution than in vacuo, and this will also be reflected on the potential energy surfaces $E(x,y)$.

In Figure 2, contours of the adiabatic potential energy surfaces $E(x,y)$ defined by eqs 1−4 are plotted for both models, assuming the product and reactant to be at equilibrium ($\eta = 0$ V). To expose the most important regions on the plot, the upper limit for the C−I bond extension y is cut at 2.5 Å; thus it does not include the area of the final dissociation. On both surfaces, the reactant well (R) with its minimum at point (0,0) corresponds to the initial state, when $n_a = 0$. It is separated from the product well (P) by the potential energy barrier, on which the saddle point (SP) has the lowest energy. The difference between the energy E(SP) and E(0,0) defines the smallest activation energy E_{act} required for the reaction. Of course, alternative reaction pathways, not through the lowest energy point, are also possible, which is known in the literature as "the saddle point avoidance phenomenon".[66−70] The potential

Table 1. Parameters Obtained for Both Models from Fitting Analytical Functions to the Results of Quantum Calculations[a]

	model VAC		
	molecule CF_3I		anion CF_3I^-
A_1	27.893279600	B_1	$0.18228176380 \times 10^{-4}$
A_2	1.259688784	B_2	3.43477084500
A_3	$-6.491947773 \times 10^{-5}$	B_3	0.49065660260
A_4	3.027538824	B_4	0.69415993040
A_5	−27.986452210	B_5	−0.49446884220
A_6	1.255608382	B_6	0.65925164610
A_7	$9.323752516 \times 10^{-2}$	B_7	−0.03086305639
		B_8	0.37969528750
d_0	4.05743	d_1	5.45980
		d_2	1.41729
	model SOLV		
	molecule CF_3I		anion CF_3I^-
A_1	15.0785201500	B_1	$4.2646514790 \times 10^{-3}$
A_2	1.1540063350	B_2	1.5843385070
A_3	$3.2740592480 \times 10^{-5}$	B_3	0.5736277134
A_4	5.8909057310	B_4	0.9926398591
A_5	−15.1812144400	B_5	−0.5801025236
A_6	1.1461867880	B_6	0.9929915636
A_7	0.1026615482		
d_0	4.05346	d_1	5.97494

[a]All values are given in au.

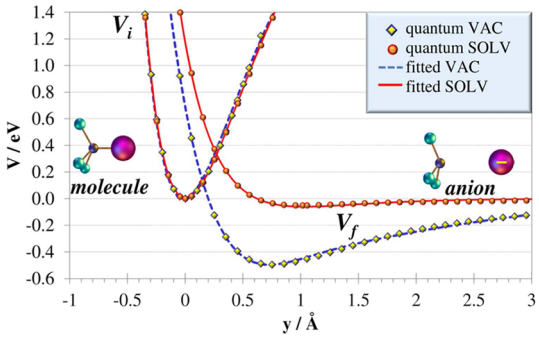

Figure 1. Potential energy profiles as a function of the C−I bond stretching obtained for the molecule (V_i) and for the anion (V_f) in the two models: VAC, fitted in the present work to the points obtained from quantum calculations in vacuo,[1] and SOLV, fitted to the points obtained from quantum calculations including solvent effect (DMSO) via the PCM model.[2]

energy surfaces shown in Figure 2a and b were obtained with Δ = 0.01 eV, which corresponds to the relatively strong reactant-metal interaction, and λ = 0.624 eV, which is equal to 25 k_BT at room temperature and was taken as a testing value.

The shape of PES, and so also the barrier height, depends on the solvent reorganization energy. For some particular solvent and the specified reactant, the λ value can be evaluated using the Marcus−Hush equation, which takes into account the static and dynamic dielectric constants of the solvent and the radius of the reactant, as described in detail in refs 71 and 72. However, the resulting energy for the heterogeneous case is rather uncertain as their magnitude may differ even by a factor of 2 due to preliminary assumptions. Therefore, in the present work, some additional tests were performed with the larger value λ = 1 eV for the solvent reorganization energy, and the shapes of these potentials are also shown in Figure 2c and d for comparison. The parameters characterizing the saddle point (SP) of the barrier on the surface $E(x,y)$ for all four cases are included in Figure 2.

As mentioned above, the potential energy surface SOLV for the overpotential η = 0 V is characterized by a much higher energy barrier than the model VAC. This implies larger overpotentials required for the reaction to proceed with an effective speed. In Figure 3, the relation between the overpotential η and the activation energy E_{act} is shown. For simplicity, the negative sign of η was omitted. In both models, an effect of larger reorganization energy λ = 1 eV is manifested not only as a shifting vertically upward of the curves $E_{act}(\eta)$ obtained with λ = 0.624 eV but also as an increasing of their slope.

3.2. Reaction Kinetics. Obviously, the effect of different activation energies must be seen in the rate constants obtained from the simulations, and this is shown in Figures 4 and 5. It should be mentioned here that, for each simulation, the uncertainty error bars by means of the 95% confidence intervals were also calculated, but they are smaller than the symbols used in our figures and so cannot be seen. Figure 4 shows that, for a given overpotential η and the same λ value, the model SOLV yields always smaller rates than the model VAC. Also the higher reorganization energy of the solvent causes the rate to decrease. As shown in Figure 5, the rate values obtained for a given activation energy with different models, but with the same parameters describing the reaction conditions, are very similar, although not identical. For most values of E_{act}, the rates obtained with the model VAC appear to be a bit higher than the results with SOLV. A clear difference is seen between the rates obtained with λ = 0.624 eV and λ = 1 eV. In the latter case, despite the same activation energy, the reaction is always slower.

From the dependence of the rate constants on the overpotentials, the electron transfer coefficient α for the reduction reaction can be calculated according to $\alpha = k_BTd\ln(k)/d\eta$. Variation of the α values with the overpotential and with the activation energy, obtained from the data shown in Figure 4, are presented in Figures 6 and 7, respectively. All four curves in Figure 6, up to a certain value of η, are practically linear, which agrees qualitatively with the Marcus theory. It is worth it to note that no clear linear tendency was observed in our earlier studies[54,55] for the electrochemical reduction of *tert*-butyl chloride and bromide molecules. Due to a very long time for simulations when the energy barriers are high, only for one case, namely with the model VAC and λ = 0.624 eV, the transfer coefficient at the equilibrium (η = 0 V) could be obtained from the simulations, and this is equal to 0.377. Linear approximation applied to three remaining curves (only in the region of small overpotentials) yields α values: 0.430 (VAC, λ = 0.624 eV), 0.573 (SOLV, λ = 0.624 eV), and 0.611 (SOLV, λ = 1 eV). Thus, the model derived from the quantum calculations in the presence of solvent predicts the transfer coefficient always above 0.5, indicating some asymmetry of the barrier on the potential surface. As can be seen additionally in Figure 6, the relationship between α and η at higher overpotentials becomes parabolic.

Interestingly, when the transfer coefficient is plotted against the activation energy (Figure 7), the differences between the two models appear to be very small. This is probably a unique feature of the CF_3I anion, for which the curvature of the potential energy profiles in vacuo and in solvent for short distances C−I is almost identical, which was shown in ref 2.

dx.doi.org/10.1021/ct400411v | J. Chem. Theory Comput. 2013, 9, 4304−4312

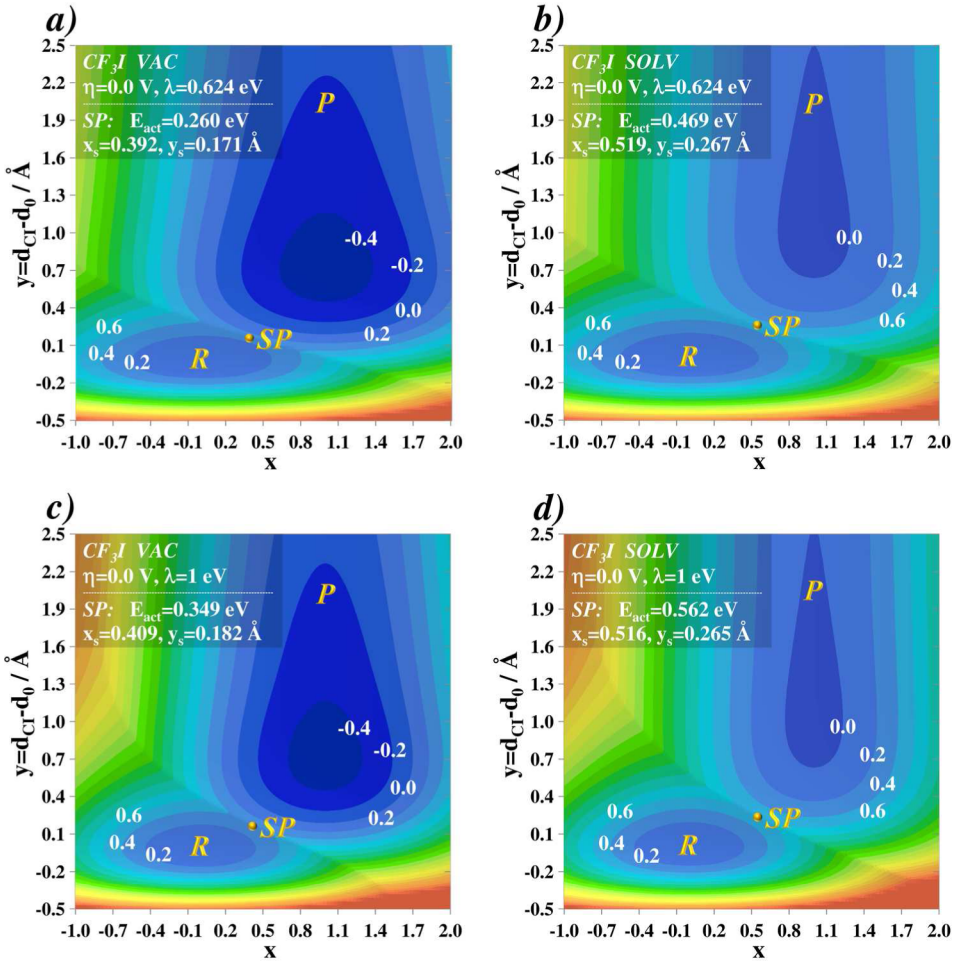

Figure 2. Contours of potential energy surfaces for the electrochemical reduction of CF_3I at equilibrium: (a and c) model VAC, (b and d) model SOLV. Parameters used in both models: Δ = 0.01 eV, (a and b) λ = 0.624 eV, (c and d) λ = 1.0 eV. For each surface, the coordinates of the saddle point (SP), x_s and y_s, and the corresponding activation energy $E_{act} = E(SP) - E_{min}(R)$ are also given.

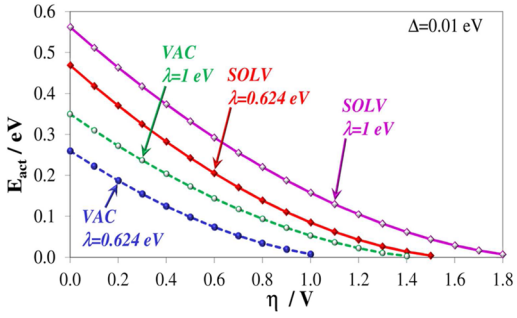

Figure 3. Activation energies (defined by the saddle point of the barrier on the potential energy surface $E(x,y)$) as a function of overpotential η, obtained for the reduction of CF_3I with the models VAC and SOLV and with two different solvent reorganization energies: λ = 0.624 eV and λ = 1.0 eV.

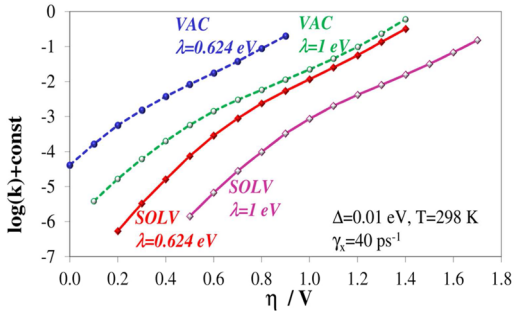

Figure 4. Rate constants obtained with models VAC and SOLV from the simulations of electrochemical reduction of CF_3I with two different solvent reorganization energies, λ = 0.624 eV and λ = 1.0 eV, as a function of overpotential.

The discrepancy in α values obtained with the two models for the same reorganization energies is larger for smaller η due to the increasing importance of the solvent reorganization in the reaction mechanism.

4. DISCUSSION

The trends observed in Figures 4 and 5 for the rate constants k obtained with different models can be explained by a possible choice of the alternative reaction paths, which may be avoiding the saddle point. The broader shape of the energy barrier on the surface, when λ is smaller, increases the probability of such phenomena. To verify this supposition, the reaction mechanism was analyzed by means of the saddle point avoidance. In this analysis, to preserve the comparative reaction conditions, the overpotential η was adjusted for each case to a value giving the same activation energy E_{act} = 0.189 eV on all four PESs. This value was used in our earlier studies on electrochemical

dx.doi.org/10.1021/ct400411v | J. Chem. Theory Comput. 2013, 9, 4304−4312

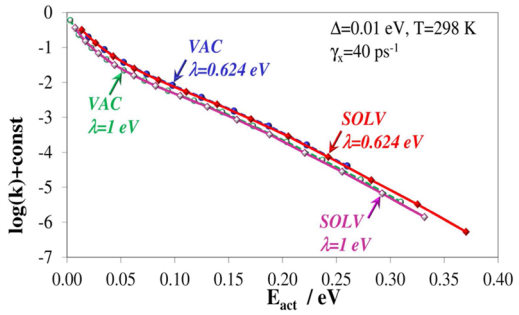

Figure 5. The rate constants obtained with different overpotentials shown as a function of activation energies.

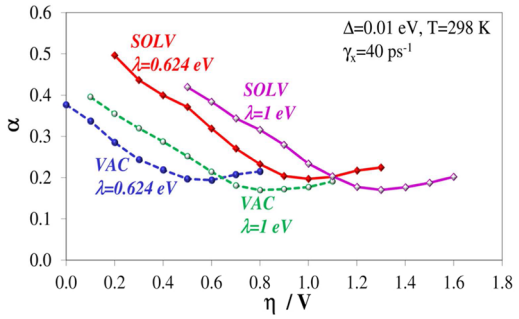

Figure 6. Dependence of the transfer coefficient α on the overpotential η, obtained with both models for two values of the solvent reorganization energy λ.

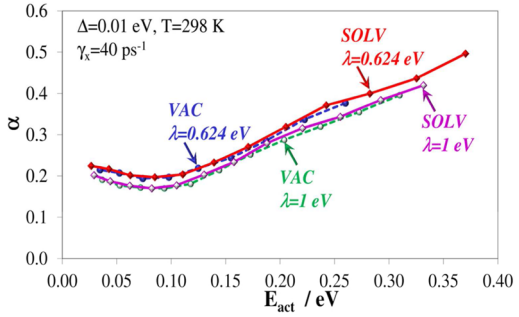

Figure 7. Relation between the transfer coefficient α and activation energies (defined by the saddle point of the potential energy barrier) resulting from application of different overpotentials.

reduction as a compromise between the accuracy of results and the computational time. Figure 8 shows the statistical distribution of coordinates x and y, collected when the occupation number reached a value higher than 0.99. As can be seen, for almost all trajectories the final points correspond to y values higher than y_s; thus the reaction occurs with the C−I bond stretched enough to reach the transition state. This is not the case for the x coordinates—in most cases, the passage from the reactant to the product area occurs with the solvent configuration intermediate between the R and SP points on the surface. The differences between the results VAC and SOLV obtained with the same λ values are very small, which explains almost identical rates observed in the simulations for the same E_{act}. However, for both λ values, maxima of the x distributions obtained with the SOLV model are closer to the saddle point. The less steep course of the curves obtained with λ = 0.624 eV explains also why this model yields higher reaction rates—the barrier shape in this case is smoother, which creates favorable

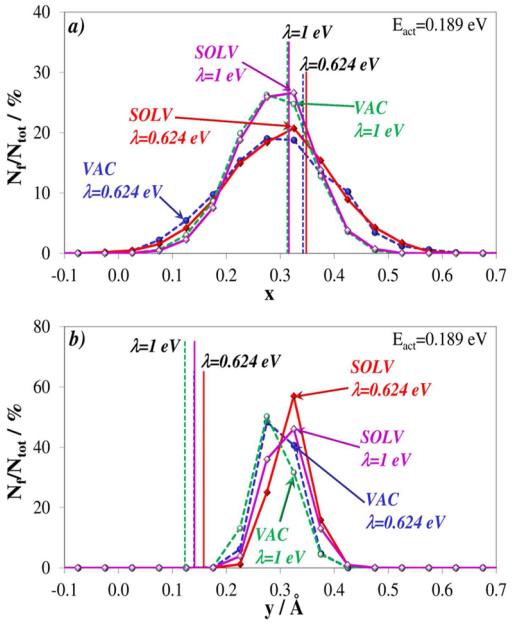

Figure 8. Statistical distribution of the final coordinates x (a) and y (b) obtained from 3000 trajectories for each model, with η chosen such that E_{act} = 0.189 eV. For both directions, the class interval of 0.05 was used. The saddle point positions on each surface are also indicated by the corresponding vertical lines.

conditions for new reaction pathways, especially in the area where $x > x_s$.

Also the alteration of the trend in $\alpha(\eta)$ from linear to parabolic, shown in Figure 6, can be explained as a manifestation of changes in the reaction mechanism: when the activation energy is small, the reaction may occur with the solvent configuration closer to the initial state than to the transition state, and crossing the barrier may occur at points farther away from the saddle point. Thus, an effect of increasing asymmetry of the barrier shape at SP due to the application of higher potentials is not seen in the transfer coefficient, because the reaction seldom proceeds via the saddle point. Indeed, the distribution of final coordinates shows that for higher overpotentials its maximum is shifted away from x_s toward x = 0. A similar effect was observed in our earlier simulations for the *tert*-butyl halides.

Some of the results presented above can be compared with those obtained experimentally by the group of Savéant.[21] The reduction of CF_3I on glassy-carbon (gc) and several metallic electrodes was investigated by the authors by cyclic voltammetry in DMF and 0.1 M NBu_4BF_4 at a low temperature T = 278 K. The reduction peak potentials E^p were found to vary strongly with the electrode material, the diminution of E^p absolute values for the metallic electrodes being assigned to the metal involvement in an inner-sphere process. Thus, the most relevant to the present studies are the results obtained for the reduction on gc. The transfer coefficient in ref 21 was calculated in the framework of the Butler-Vomer rate law. The reduction of CF_3I occurred at a potential of about −1.52 V, and the transfer coefficient was found to range from 0.26 to 0.3, depending on the measurement procedure. The authors used also the theoretical model of Savéant,[64] in which the solvent reorganization energy of λ = 0.52 eV was assumed, and obtained the value of 0.34.

dx.doi.org/10.1021/ct400411v | J. Chem. Theory Comput. 2013, 9, 4304−4312

The transfer coefficient value of 0.26 reported from the experiment according to eq 1 in ref 21 corresponds to the midpoint E_m between the peak and the half-peak potential, which is approximately equal to −1.44 V. The difference between E_m and the rough estimate of −0.54 V for the standard potential E°[21] yields an approximate value of 0.9 V (minus is omitted) for the overpotential. As can be seen in Figure 6, with the model VAC and λ = 0.624 eV, the overpotential of 0.9 V is unattainable, while with λ = 1 eV, this model yields α = 0.172, which is much smaller than the lowest limit of 0.26 suggested in ref 21. This confirms that the model VAC is insufficient for the description of the real system. Higher values are obtained with the model SOLV, which for λ = 0.624 eV gives α = 0.204, while for λ = 1 eV, α = 0.28. The latter value is identical with the result derived from the formula 1 in ref 21; thus, among four tested models, the most accurate appears to be the model SOLV (λ = 1 eV).

The comparisons presented above suggest that the higher λ value of 1 eV properly describes the solvent reorganization for the electrochemical reduction of the CF_3I molecule, and thus the estimate of 0.52 eV, derived in the work of Savéant from the Marcus dielectric continuum model, underestimates it. However, this hypothesis should be treated with caution. One should remember about several important differences between the theoretical and experimental approaches, which make their comparison quite difficult and uncertain. First of all, the theoretical model used in the present work by default isolates the process from any other interfering phenomena occurring in the experiment, such as competitive reactions, including adsorption on the metal surface. The systems are therefore different by nature, so the correspondence of results is very difficult to achieve. Also, our evaluation of overpotential corresponding to the experimental conditions is rather crude, based on the rough estimate of standard potential given in ref 21. As shown in Figure 6, for the SOLV model the decrease of overpotential from 0.9 to 0.8 V causes a significant increase in the transfer coefficient, which for the latter reaches values of 0.232 when λ = 0.624 eV and 0.316 when λ = 1 eV. A different value taken for the friction coefficient γ_x, which in all above simulations was assumed to be equal to 40 ps^{-1}, may also influence the results, although it is not expected to play a very significant role.[54]

Another possible source of discrepancy might be the temperature. All simulations in the present work were performed at room temperature, while the measurements were conducted at T = 278 K. In our earlier studies on *tert*-butyl halides,[56] it was shown that the transfer coefficient may vary with the temperature, although the change is not expected to be large when cooling the system by only 20 K. Indeed, additional simulations performed for the CF_3I system with the SOLV model in 278 K and for η = 0.9 V gave α = 0.204 for λ = 0.624 eV and α = 0.283 for λ = 1 eV. The first value is the same as that obtained at T = 298 K, while the second is a bit larger than the corresponding 0.28. Thus, the temperature effect on the transfer coefficient for the reduction of CF_3I appears to vary with the solvent reorganization energy, which may be related to different heights of the barrier on the potential energy. More thorough studies on this phenomenon will be undertaken in the near future.

5. CONCLUSIONS

As shown in the present work, the models VAC and SOLV give very different rate constants and transfer coefficients with respect to overpotentials but exhibit also some qualitative similarities. The latter are due to a particular feature of trifluoromethyl iodide, namely almost identical slopes of its potential energy profiles for the neutral and anionic forms near their crossing point obtained from quantum calculations without and with solvent. Therefore, the same tendencies in the kinetics are shown by both models. They give also very similar values for the reaction rates and transfer coefficients with respect to the activation energy.

The quantitative discrepancies between the results VAC and SOLV are mainly manifested in shifting the rates SOLV toward higher overpotentials by about 0.44 V, which is the energy difference between minima of anionic curves shown in Figure 1. It can be therefore concluded that the model based on the quantum calculations in vacuo can serve only for approximate estimation of general tendencies. Thus, for some purposes, the phenomena of vanishing of the minimum on the anionic curve in the solution can be ignored. However, the results cannot be then directly related to the overpotentials observed in the experiment. Also, one should note that even if the shift of η is taken into account, some quantitative differences exist in the results for smaller overpotentials, indicating the importance of the inclusion of the solvent effect into the quantum calculations. It is worth it to mention here that, as shown in ref 2, the Morse potential used in the model of Savéant for the interaction between the radical $CF_3^{\bullet}$ and anion I^- in solution is more repulsive and less steep for small C−I distances than predicted by the quantum calculations in the solvent, which leads to overestimation of both the activation energy and transfer coefficient.

The results obtained in the present work with the SOLV model show strong variation of the transfer coefficient α with overpotentials corresponding to high activation energies. This is an average effect of modification of the shape of the potential energy barrier upon η and coincident change in the reaction mechanism. For smaller E_{act} (high overpotentials), the reaction may occur with the solvent configuration close to the initial state, and in this region the transfer coefficient is rather weakly dependent on η.

The transfer coefficient is found to depend strongly also on the solvent reorganization energy λ. The value of α = 0.204 obtained with the model SOLV for η = 0.9 V and λ = 0.624 eV is significantly smaller than the lower limit of 0.26 reported from the experiment, while perfect agreement (α = 0.28) is achieved with λ = 1 eV. This leads to the conclusion that the model SOLV (λ = 1 eV) best reproduces the interplay of various factors which are the most important in the actual process of electrochemical reduction of the CF_3I molecule.

AUTHOR INFORMATION

Corresponding Author

*Phone: (+48 42) 635 57 91. E-mail: anignacz@uni.lodz.pl.

Notes

The authors declare no competing financial interest.

REFERENCES

(1) Ignaczak, A.; Łaszczych, B. DFT Study on the One-Electron Reduction of CF_3X (X═Cl, Br, I) Molecules. *Comput. Theor. Chem.* **2011**, *966*, 340−351.

(2) Ignaczak, A. Solvent Effect on the Potential Energy Surfaces for the One-Electron Reduction of CF3X (X═Cl, Br, I) Molecules: A DFT PCM Study. *J. Phys. Chem. A* **2012**, *116*, 11694−11701.

(3) Sibille, S.; Mcharek, S.; Périchon, J. Electrochemical Trifluoromethylation of Carbonyl Compounds. *Tetrahedron* **1989**, *45*, 1423−1428.
(4) Vecchio-Sadus, A. M. The Electrochemical Synthesis of Inorganic and Organometallic Complexes in Non-Aqueous Media. *J. Appl. Electrochem.* **1993**, *23*, 401−416.
(5) Aymard, F.; Nédélec, J.-Y.; Périchon, J. An Efficient Inexpensive Electrochemical Preparation of Ruppert's Reagent. *Tetrahedron Lett.* **1994**, *35*, 8623−8624.
(6) Paratian, J. M.; Labbé, E.; Sibille, S.; Nédélec, J.-Y.; Périchon, J. Electrochemical Synthesis of Trifluoromethylcadmium and Trifluoromethylzinc Species Using Bromotrifluoromethane and Sacrificial anodes. *J. Organomet. Chem.* **1995**, *487*, 61−64.
(7) Paratian, J. M.; Labbé, E.; Sibille, S.; Périchon, J. Electrosynthesis of (Trifluoromethyl)copper Complexes from Bromotrifluoromethane: Reactivities with Various Organic Halides. *J. Organomet. Chem.* **1995**, *489*, 137−143.
(8) Fuchigami, T. Electrochemistry Applied to Synthesis of Fluorinated Organic Substances. In *Advances In Electron Transfer Chemistry*; Mariano, P., Ed.; JAI Press: Greenwich, CT, 1999; Vol. *6*, pp 41−130.
(9) Koshechko, V. G.; Kiprianova, L. A. Electrochemically Activated Insertion of Fluoroalkyl Groups into Organic and Inorganic Substrates. *Theor. Exp. Chem.* **1999**, *35*, 18−36.
(10) Koshechko, V. G.; Pokhodenko, V. D. Electrochemical Activation of Freons Using Electron transfer Mediators. *Russ. Chem. Bull., Int. Ed.* **2001**, *50*, 1929−1935.
(11) Singh, R. P.; Shreeve, J. M. Nucleophilic Trifluoromethylation Reactions of Organic Compounds with (Trifluoromethyl)-trimethylsilane. *Tetrahedron* **2000**, *56*, 7613−7632.
(12) Sonoyama, N.; Sakata, T. Electrochemical Hydrogenation of CFC-13 Using Metal-Supported Gas Diffusion Electrodes. *Environ. Sci. Technol.* **1998**, *32*, 4005−4009.
(13) Sonoyama, N.; Sakata, T. Conversion of CFC-13 to Trifluoroacetic Acid by Electrochemical Reaction with Carbon Dioxide. *Chem. Lett.* **2002**, *31*, 444−445.
(14) Lyon, J. T.; Andrews, L. Group 4 Metal Atom Reactions with CF_3Cl, $CFCl_3$, CF_3Br, and CF_3I: A Matrix Infrared Spectroscopic and DFT Investigation of Competitive α-Halogen Transfer to Form Triplet $XC{\div}MX_3$ Complexes. *Organometallics* **2007**, *26*, 4152−4159.
(15) Ma, J.-A.; Cahard, D. Strategies for Nucleophilic, Electrophilic, and Radical trifluoromethylations. *J. Fluorine Chem.* **2007**, *128*, 975−996.
(16) Grobe, J.; Hegge, J. Electrochemical and Chemical Syntheses of Trifluoromethylating Reagents and Trifluoromethyl Substituted Compounds. *Z. Anorg. Allg. Chem.* **2008**, *634*, 1975−1990.
(17) Murphy, P. M.; Baldwin, C. S.; Buck, R. C. Syntheses Utilizing n-Perfluoroalkyl Iodides [R_FI, C_nF_{2n+1}-I] 2000−2010. *J. Fluorine Chem.* **2012**, *138*, 3−23.
(18) Andrieux, C. P.; Savéant, J.-M.; Su, K.-B. Kinetics of Dissociative Electron Transfer. Direct and Mediated Electrochemical Reductive Cleavage of the Carbon-Halogen Bond. *J. Phys. Chem.* **1986**, *90*, 3815−3823.
(19) Andrieux, C. P.; Gallado, I.; Savéant, J.-M.; Su, K.-B. Dissociative Electron Transfer. Homogeneous and Heterogeneous Reductive Cleavage of the Carbon-Halogen Bond in Simple Aliphatic Halides. *J. Am. Chem. Soc.* **1986**, *108*, 638−647.
(20) Andrieux, C. P.; Gallado, I.; Savéant, J.-M. Outer-Sphere Electron-Transfer Reduction of Alkyl Halides. A Source of Alkyl Radicals or of Carbanions? Reduction of Alkyl Radicals. *J. Am. Chem. Soc.* **1989**, *111*, 1620−1626.
(21) Andrieux, C. P.; Gélis, L.; Médebielle, M.; Pinson, J.; Savéant, J.-M. Outer-Sphere Dissociative Electron Transfer to Organic Molecules: A Source of Radicals or Carbanions? Direct and Indirect Electrochemistry of Perfluoroalkyl Bromides and Iodides. *J. Am. Chem. Soc.* **1990**, *112*, 3509−3520.
(22) Médebielle, M.; Pinson, J.; Savéant, J.-M. Electrochemically Induced Nucleophilic Substitution of Perfluoroalkyl Halides. An Example of a Dissociative Electron-Transfer-Induced Chemical Reaction. *J. Am. Chem. Soc.* **1991**, *113*, 6872−6879.
(23) Médebielle, M.; Pinson, J.; Savéant, J.-M. Electrochemically Induced Nucleophilic Substitution of Perfluoroalkyl Halides: an Example of a Dissociative Electron-Transfer-Induced Chemical Reaction. *J. Fluorine Chem.* **1992**, *58*, 254.
(24) Bertran, J.; Gallardo, I.; Moreno, M.; Savéant, J.-M. Dissociative Electron Transfer. Ab Initio Study of the Carbon-Halogen Bond Reductive Cleavage in Methyl and Perfluoromethyl Halides. Role of the Solvent. *J. Am. Chem. Soc.* **1992**, *114*, 9576−9583.
(25) Andrieux, C. P.; Le Gorande, A.; Savéant, J.-M. Electron Transfer and Bond Breaking. Examples of Passage from a Sequential to a Concerted Mechanism in the Electrochemical Reductive Cleavage of Arylmethyl Halides. *J. Am. Chem. Soc.* **1992**, *114*, 6892−6904.
(26) Andrieux, C. P.; Savéant, J.-M.; Tardy, C. Cage and Entropy Effects in the Dynamics of Dissociative Electron Transfer. *J. Am. Chem. Soc.* **1998**, *120*, 4167−4175.
(27) Costentin, C.; Robert, M.; Savéant, J.-M. Successive Removal of Chloride Ions from Organic Polychloride Pollutants. Mechanisms of Reductive Electrochemical Elimination in Aliphatic Gem-Polychlorides, α,β-Polychloroalkenes, and α,β-Polychloroalkanes in Mildly Protic Medium. *J. Am. Chem. Soc.* **2003**, *125*, 10729−20739.
(28) Rozhkov, I.; Becker, G.; Igumnov, S.; Pletnev, S.; Rempel, G.; Borisov, Y. Reduction Potential and Relative Electron Affinity As reactivity Indexes of Perfluoroalkyl Halides. *J. Fluorine Chem.* **1989**, *45*, 114.
(29) Volodin, Yu. Yu.; Stepanov, A. A.; Denisovich, L. I.; Grinberg, V. A. Electrocatalytic Reduction of Trifluoroiodomethane in the Presence of Cobaloximes. *Russ. J. Electrochem.* **2000**, *36*, 1026−1028.
(30) Shimizu, Y.; Ueda, K.; Chiba, H.; Okunishi, M.; Ohmori, K.; Sato, Y.; Suzuki, I. H.; Ibuki, T.; Okada, K. Auger Electron Spectra of CF_3CN, CF_3Cl, CF_2Cl_3 and $CFCl_3$. *Chem. Phys.* **1999**, *244*, 439−448.
(31) Batanov, G. M.; Kossyi, I. A.; Silakov, V. P. Gas-Discharge Method for Improving the Environmental Characteristics of the Atmosphere (In memory of G.A. Askar'yan). *Plasma Phys. Rep.* **2002**, *28*, 204−228.
(32) Miller, T. M.; Friedman, J. F.; Schaffer, L. C.; Viggiano, A. A. Electron Attachment to Halomethanes at High Temperature: CH_2Cl_2, CF_2Cl_2, CH_3Cl, and CF_3Cl Attachment Rate Constants up to 1100 K. *J. Chem. Phys.* **2009**, *131*, 84302.
(33) Wilde, R. S.; Gallup, G. A.; Fabrikant, I. I. Semiempirical *R*-Matrix Theory of Low Energy Electron−CF_3Cl Inelastic Scattering. *J. Phys. B* **1999**, *32*, 663−673.
(34) Fabrikant, I. I.; Hotop, H. On the Validity of the Arrhenius Equation for Electron Attachment Rate Coefficients. *J. Chem. Phys.* **2008**, *128*, 124308.
(35) Roszak, S.; Koski, W. S.; Kaufman, J. J.; Balasubramanian, K. Structure and Energetics of CF_3Cl^-, CF_3Br^-, and CF_3I^- Radical Anions. *J. Chem. Phys.* **1997**, *106*, 7709−7713.
(36) Roszak, S.; Koski, W. S.; Kaufman, J. J.; Balasubramanian, K. Structure and Electron Attachment Properties of Halomethanes (CXnYm, X=H, F; Y=Cl, Br, I; n=0,4; m=4-n). *SAR QSAR Environ. Res.* **2000**, *14*, 1−15.
(37) Berry, R. J.; Burgess, D. R. F., Jr.; Nyden, M. R.; Zachariah, M. R.; Melis, C. F.; Schwartz, M. Halon Thermochemistry: Calculated Enthalpies of Formation of Chlorofluoromethanes. *J. Phys. Chem.* **1996**, *100*, 7405−7410.
(38) Luke, B. T.; Loew, G. H.; McLean, A. D. Theoretical Investigation of the Anaerobic Reduction of Halogenated Alkanes by Cytochrome P-450. 2. Vertical Electron Affinities of Chlorofluoromethanes as a Measure Their Activity. *J. Am. Chem. Soc.* **1988**, *110*, 3396−3400.
(39) Gutsev, G. L. Density Functional Investigation on the Electron Affinity of the CF_nCl_m series, n+m=3 and 4. *J. Chem. Phys.* **1993**, *98*, 7072−7080.
(40) Beyer, T.; Nestmann, B. M.; Peyerimhoff, S. D. Study of Electron Polarization and Correlation Effects in Resonant and Background Electron Scattering of CF_3Cl. *Chem. Phys.* **2000**, *255*, 1−14.

(41) Fernandez, L. E.; Varetti, E. L. Scaled Quantum Mechanical Force Fields for the Isoelectronic Molecules CF_3X (X = SiH_3, PH_2, SH, Cl). *Z. Anorg. Allg. Chem.* **2007**, *633*, 2678−2682.
(42) Rempel, G. D.; Borisov, Yu.A.; Raevskii, N. I.; Igumnov, S. M.; Rozhkov, I. N. Electron Structure and Reactivity of Organofluorine Compounds. 3. MNDO and AM1 Calculations of the Ground State of Perfluoroalkyl Chlorides, Bromides, and Iodides. *Russ. Chem. Bull.* **1990**, *39*, 947−950.
(43) Rempel, G. D.; Borisov, Yu.A.; Raevskii, N. I.; Igumnov, S. M.; Rozhkov, I. N. Electron Structure and Reactivity of Organofluorine Compounds. 4. AM1 Calculations of Anion Radicals of Primary, Secondary, and Tertiary Perfluoroalkyl Chlorides, Bromides, and Iodides. *Russ. Chem. Bull.* **1990**, *39*, 951−955.
(44) Bettega, M. H. F.; Natalense, A. P. P.; Lima, M. A. P.; Ferreira, L. G. Elastic Scattering of Low-Energy Electrons by CF_3Cl, CF_3Br and CF_3I. *J. Phys. B* **2003**, *36*, 1263−1272.
(45) Abraham, R. J.; Griffith, L.; Loftus, P. Approaches to Charge Calculations in Molecular Mechanics. *J. Comput. Chem.* **1982**, *3*, 407−416.
(46) Abraham, R. J.; Grant, G. H. Charge Calculations in Molecular Mechanics. IX. A General Parameterisation of the Scheme for Saturated Halogen, Oxygen and Nitrogen Compounds. *J. Comput.-Aided Mol. Des.* **1992**, *6*, 273−286.
(47) Pezler, B.; Szamrej, I. Geometry and energy changes in halomethanes due to electron capture. *Res. Chem. Intermed.* **2001**, *27*, 787−794.
(48) Senthilkumar, K.; Kolandaivel, P. Hartree-Fock and Density Functional Theory Studies on Ionization and Fragmentation of Halomethane Molecules by Positron Impact. *Mol. Phys.* **2002**, *100*, 3817−3822.
(49) Preston, H. J. T.; Kaufman, J. J. MS Xα Calculations on the Chlorofluoromethanes. *Chem. Phys. Lett.* **1977**, *50*, 157−161.
(50) Komiha, N.; Kabbaj, O. K.; Lhamyani-Chraibi, M. Theoretical Study of the Electron Attachment Dissociation of Methyl Halides and Freon Molecules: CF_3Cl, CF_2Cl_2, $CFCl_3$. *J. Fluorine Chem.* **2001**, *108*, 177−186.
(51) German, E. D.; Tikhomirov, V. A. A Semiempirical Study of Radical Anions $CY3X^{\pm}$ (Y=H, F, Cl and Br, X═Cl and Br). *J. Mol. Struct.: THEOCHEM* **1998**, *423*, 251−261.
(52) Tikhomirov, V. A.; German, E. D. Dissociative Electron Transfer to Polyhalogen Methanes CY_3X (Y_=H, F, Cl and Br; X═Cl and Br) in solvent: a semiempirical PM3 method Study. *J. Electroanal. Chem.* **1998**, *450*, 13−20.
(53) Ignaczak, A.; Schmickler, W. Theoretical Study of a Non-Adiabatic Dissociative Electron Transfer Reaction. *J. Electroanal. Chem.* **2003**, *554*−*555*, 201−209.
(54) Ignaczak, A.; Schmickler, W. MD Simulations of Heterogeneous Reduction of the Tert-Butyl Bromide Molecule. *Electrochim. Acta* **2010**, *55*, 2442−2450.
(55) Ignaczak, A. Electrochemical Reduction of Tert-Butyl Chloride—Computational Study. *Electrochim. Acta* **2010**, *55*, 3650−3656.
(56) Ignaczak, A. Comparison of Temperature Effect on Electroreduction of Tert-Butyl Chloride and Tert-Butyl Bromide—Theoretical Study. *Electrochim. Acta* **2011**, *56*, 6305−6311.
(57) Koper, M. T. M.; Voth, G. A. A Theory of Adiabatic Bond Breaking Electron Transfer Reactions at Metal Electrodes. *Chem. Phys. Lett.* **1998**, *282*, 100−106.
(58) Schmickler, W.; Koper, M. T. M. Adiabatic Electrochemical Electron-Transfer Reactions Involving Frequency Changes of Inner-Sphere Modes. *Electrochem. Commun.* **1999**, *1*, 402−405.
(59) Kast, S. M.; Nicklas, K.; Bär, H.-J.; Brickmann, J. Constant Temperature Molecular Dynamics Dimulations by Means of a Stochastic Collision Model. I. Noninteracting Particles. *J. Chem. Phys.* **1994**, *100*, 566−576.
(60) Kast, S. M.; Brickmann, J. Constant Temperature Molecular Dynamics Simulations by Means of a Stochastic Collision Model. II. The Harmonic Oscillator. *J. Chem. Phys.* **1996**, *104*, 3732−3741.
(61) Ignaczak, A.; Schmickler, W. Effects of Friction and Asymmetric Inner Sphere Reorganization Energy on the Electron Transfer Reaction Rate—Two-Dimensional Simulations. *Electrochim. Acta* **2007**, *52*, 5621−5633.
(62) Ignaczak, A. Adiabatic Versus Non-Adiabatic Approach to the Inner Sphere Vibrational Effects on Electrochemical Reduction Rates. *Electrochim. Acta* **2008**, *53*, 2619−2629.
(63) Whitnell, R. M.; Wilson, K. R.; Hynes, J. T. Vibrational Relaxation of a Dipolar Molecule in Water. *J. Chem. Phys.* **1992**, *96*, 5354−5369.
(64) Murarka, R. K.; Bhattacharyya, S.; Biswas, R.; Bagchi, B. Isomerization Dynamics in Viscous Liquids: Microscopic Investigation of the Coupling and Decoupling of the Rate to and from Solvent Viscosity and Dependence on the Intermolecular Potential. *J. Chem. Phys.* **1999**, *110*, 7365−7375.
(65) Bagchi, A.; Srinivas, G.; Miyazaki, K. The Enskog Theory for Classical Vibrational Energy Relaxation in Fluids with Continuous Potentials. *J. Chem. Phys.* **2001**, *115*, 4195−4198.
(66) Northrup, S. H.; McCammon, J. A. Saddle-Point Avoidance in Diffusional Reactions. *J. Chem. Phys.* **1983**, *78*, 987−989.
(67) Berkowitz, M.; Morgan, J. D.; McCammon, J. A.; Northrup, S. H. Diffusion-Controlled Reactions: A Variational Formula for the Optimum Reaction Coordinate. *J. Chem. Phys.* **1983**, *79*, 5563−5565.
(68) Larson, R. S. Simulation of Two-Dimensional Diffusive Barrier Crossing with a Curved Reaction Path. *Physica A* **1986**, *137*, 295−305.
(69) Berezhkovskii, A. M.; Berezhkovskii, L. M.; Zitserman, V. Yu. The Rate Constant in the Kramers Multidimensional Theory and the Saddle-Point Avoidance. *Chem. Phys.* **1989**, *130*, 55−63.
(70) Berezhkovskii, A. M.; Zitserman, V. Yu.; Sheu, S.-Y.; Yang, D.-Y.; Kuo, J.; Lin, S. H. Kramers Theory of Chemical Reactions in a Slowly Adjusting Environment. *J. Chem. Phys.* **1997**, *107*, 10539−10554.
(71) Savéant, J.-M. A Simple Model for the Kinetics of Dissociative Electron Transfer in Polar Solvents. Application to the Homogeneous and Heterogeneous Reduction of Alkyl Halides. *J. Am. Chem. Soc.* **1987**, *109*, 6788−6795.
(72) Savéant, J.-M. Dissociative Electron Transfer. New Tests of the Theory in the Electrochemical and Homogeneous Reduction of Alkyl Halides. *J. Am. Chem. Soc.* **1992**, *114*, 10595−10602.